Wind Fields at the Sea Surface Determined from Combined Ship and Satellite Altimeter Data

JACQUES SERVAIN

Centre ORSTOM, Brest, France

FRANCIS GOHIN

Département d'Océanographie Spatiale, IFREMER, Brest, France

ALAIN MUZELLEC*

Ecole Nationale de la Météorologie, Toulouse, France

(Manuscript received 23 December 1992, in final form 14 April 1993)

ABSTRACT

A data processing method based on a kriging technique was developed to merge two data sources relative to wind velocity at the sea surface within a basin-scale region (the tropical Atlantic Ocean): one from in situ wind observations in a ships of opportunity network and the other from satellite measurements involving reconstructions of wind velocity from the Geosat altimeter signal. The kriging parameters used are computed and discussed. The high density of the combined ship–satellite data files allowed the integrated time step to be reduced from one month to 10 days. To illustrate the method, resulting wind velocity patterns are given for three 10-day running periods. The technique was validated at monthly and 10-day time periods by comparison with independent data processing sources involving only in situ observations or Geosat measurements. Work is now in progress to extend this method to wind vectors supplied by the scatterometer boarded on the *ERS-1* satellite.

1. Introduction

Progress in understanding climatic variability requires a better evaluation of meteorological parameters at the air–sea interface. Among these parameters, the wind field is of prime importance for empirical studies and numerical experiments relative to oceanic circulation on a basin scale. This is notably the case in tropical regions where ocean response to atmospheric forcing is particularly rapid and impressive. Wind stress is of first importance as a driving force for running oceanic general circulation models (OGCMs). Moreover, the thermal forcing of the ocean, related to turbulent heat flux components at the air–sea interface as well as to ocean–atmosphere CO_2 gas fluxes, depends largely on wind velocity.

The spatial resolution of OGCMs is about 100 km (occasionally less, e.g., along the equator and coasts), and the integration step is generally hourly (e.g., Andrich et al. 1988). Obviously, current technology for gathering marine wind observations is unsatisfactory for such fine space–time resolution. Until recently, the only possibility for mapping observed wind fields was to use marine weather reports collected by selected ships navigating across the oceans. In spite of the limitations inherent in this observational procedure (e.g., spatial data density related largely to the main shipping lanes, errors in measurements and/or data transmission, etc.), these wind observations were, and still are, very useful to climate studies. Moreover, in recent years, there has been renewed interest in this approach because of a continual increase in the real-time transmission rate. However, the number of weather reports has remained limited, especially in the southern oceans. Consequently, it is still impossible, at least on an oceanic basin scale, to analyze wind fields at time steps of less than one month. Undeniably, this is a serious handicap to improving knowledge of the effect of synoptic wind fields on the ocean.

In the future, wind data derived from satellite observations will undoubtedly provide additional, very detailed information. "Satellite wind" is in fact a sea surface wind estimation reconstructed from the state of the oceanic surface, which is itself measured by satellite instruments such as microwave radiometers, altimeters, and scatterometers. The two first-mentioned

* Current affiliation: SCEM/MAR, Météo-France, Toulouse, France.

Corresponding author address: Dr. Jacques Servain, Centre ORSTOM de Brest, BP 70, Plouzané, France 29280.

instruments supply only the modulus of the wind, as in the case of the altimeter boarded on Geosat during 1984–89. The scatterometer provides both wind components, but such data has only been available in an operational mode since 1991, thanks to satellite *ERS-1*. The reconstruction of sea surface wind is done with empirical models, which on the whole provide reasonable results. However, there can be difficulties in cases of very high (>20 m s^{-1}) or very slow (<4 m s^{-1}) wind speeds (Etcheto and Banège 1992).

One great advantage of the satellite as compared to weather reports is the instant availability and enormous space–time density of the data, which should allow determination of synoptical wind fields at less than monthly time steps.

One obvious operating procedure would be to construct wind fields solely from satellite data. However, our intention was to test the feasibility of constructing wind fields from an appropriate management of both satellite and ship datasets. In our opinion, this approach has three advantages:

(i) all wind observations available within a delimited area during a given period are used, regardless of the type of information;
(ii) deficiencies in one type of data are more or less compensated by the quality of other types;
(iii) management of satellite–ship datasets should ensure better continuity in conducting multiyear time series previously based only on ship data.

The numerical procedure used here to merge satellite and ship wind data is based on geostatistical methods. Since this work was exploratory, the study was deliberately simplified and the space and time conditions limited.

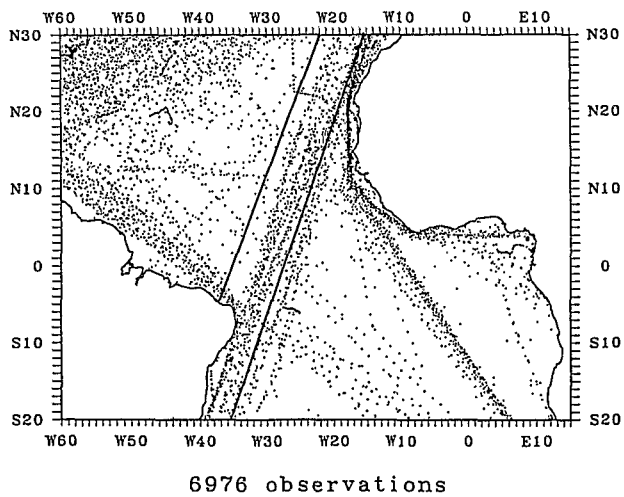

FIG. 1. An example (February 1992) of monthly distribution derived from surface observations provided by ships of opportunity in real time on the GTS. Note the two oblique lines surrounding the high density of data along the Europe–South America shipping route.

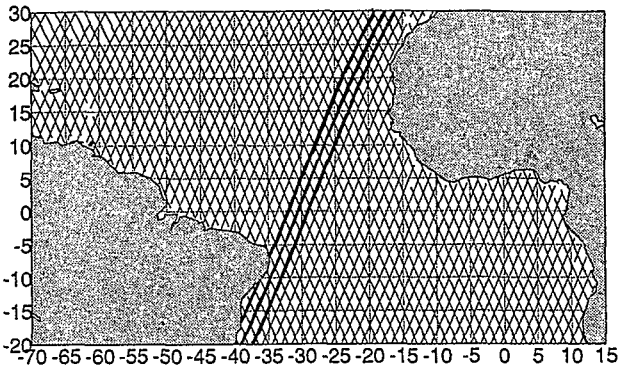

FIG. 2. An example (cycle 3 from 12 December to 29 December 1986) of Geosat tracks. Note that three tracks are very close to the Europe–South America shipping route (see Fig. 1).

As we used wind modulus data provided by the Geosat altimeter, the wind direction component could not be taken into account. Wind velocity data supplied by marine weather reports transmitted in real time on the Global Telecommunication System (GTS) supplemented satellite wind information. Our study was limited in space to one oceanic basin, that is, the tropical Atlantic Ocean, which is our usual monitoring area (Servain 1990). The study was also limited in time since the geostatistical coefficients used in implementing the computational method were estimated over a 12-month working period, and the wind data–merging procedure was performed during a 1-month test period.

The paper is structured as follows: Brief information about the datasets used is given in section 2. The computational method is then developed in section 3 and the wind patterns related to the test period discussed in section 4. A conclusion and statement about future work are provided in section 5.

2. Data

a. In situ data

Monthly time series of 2° latitude × 2° longitude averages and anomalies of pseudo–wind stress (wind components times wind magnitude) have been edited and regularly updated (Picaut et al. 1985; Servain et al. 1987; Servain and Lukas 1990, hereafter SL; BOAT's collection 1990–91). In addition to their interest for ocean modeling (Morlière and Duchêne 1991; Servain et al. 1992), these time series are important for climatic change studies (Picaut et al. 1984; Servain and Legler 1986). Originally, raw data were provided, with a minimum 6-month delay, by the National Climatic Data Center (NCDC). Now, wind data collected by ships of opportunity are routed monthly to our computer facilities via the international network (Servain 1990). About 7000 observations per month are available over the study area. An example of monthly data distribution is given in Fig. 1. As noted above, large spatial irregularities appear in the data sampling.

b. Geosat data

Geosat data were collected during the Exact Repeat Mission (ERM) between October 1986 and September 1989. For that mission, the Geosat repeat cycle (the time separating the quasi-coincidence of two tracks on the earth surface) was 17 days. One cycle was composed of 245 revolutions around the earth. Two adjacent tracks were separated by about three days and spaced by 164 km at the equator (Fig. 2). Alongtrack spacing was 6.8 km, corresponding to 1-s averages on the geophysical data records [see Cheney et al. (1987) for more details].

Several algorithms have been proposed to compute wind velocity 10 m from the near-nadir radar cross section σ_0 provided by a satellite altimeter (e.g., Brown 1979; Goldhirst and Dobson 1985; Chelton and Wentz 1986; Dobson et al. 1987; Witter and Chelton 1991). Wind calibration is generally achieved using ship and buoy measurements as references. The quality of each algorithm can differ depending on the oceanic region and the time scale for averaging data (e.g., Boutin 1990; Etcheto and Banège 1992). In our case, a preliminary statistical study (Muzellec 1991) led to selection of the algorithm proposed by Chelton and Wentz (1986).

3. Computational method

Geostatistical techniques, especially the interpolation method known as kriging (Matheron 1971), were introduced in oceanographic studies 20 years ago (Olea 1974). The method used here to merge wind measurements is derived from an extension to time averaging of a study proposed for sea surface temperature (Gohin and Langlois 1993). By kriging, we estimate the wind values on a regular grid (in space and time), taking into account the available dataset in the vicinity of each node. The local estimators are linear combinations of observed measurements whose weights depend on their origin (in situ or satellite) and the distance between time–space locations. The optimal interpolation fulfills both a condition of nonbias and a condition of minimum error.

For statistical modeling of the kriging error we set hypotheses through two main assumptions, respectively, linked to the raw error and the spatiotemporal correlation of the wind measurements:

- The first assumption deals with (i) variance of in situ measurements and (ii) variance of Geosat measurements, the latter being subdivided into two terms, that is, true white noise and correlated noise along the same track.
- The second assumption concerns the spatiotemporal structure schematized by the existence of the variogram of wind velocity V considered as a random function

$$\gamma_{(\Delta h,\Delta t)} = 1/2E[V_{(x+\Delta h,t+\Delta t)} - V_{(x,t)}]^2,$$

where Δh and Δt are space and time increments, respectively, and E is the statistical mean. This implies that the variance of the difference $[V_{(x+\Delta h,t+\Delta t)} - V_{(x,t)}]$ depends on the distances between their space–time locations (Δh, Δt) and does not depend only on their space locations.

The space–time variogram is expressed as an exponential function:

$$\gamma_{(x,t)} = \omega\left\{1 - \exp\left[-\frac{1}{a}(x + bt)\right]\right\} \qquad (1)$$

where ω is the sill value, a is the space range, and a/b is the time range.

Note that spatial isotropy of the signal is assumed, which is obviously an approximation of reality.

Experimentally, the variogram components were first estimated separately for each type of wind data and then on a mixed set of wind data. Such a study is more precise if based on ship and satellite data closely related in both time and space. For that purpose, we used a particularity of Geosat orbits previously exploited by others (Arnault et al. 1992). Three descending tracks (Fig. 2) pass alongside the main shipping lane between Europe and South America (see Fig. 1). Due to technical problems (i.e., stability of the satellite platform, etc.), all Geosat tracks were not always fully sampled. In view of the density of wind information supplied by the three tracks during ERM, we selected a one-year-long period (1 October 1988–29 September 1989) overlying cycles 41 to 62 (Fig. 3). During this one-year period, around 250 000 satellite wind data were available. This number is to be compared with roughly 11 000 ship wind data observed during the same time period within the two oblique lines straddling the Europe–South America shipping route (see Fig. 1). A time–space study performed for these observations (Muzellec 1991) indicated that 633 satellite–ship data pairs corresponded simultaneously to a distance of less than 200 km and a time span of less than 6 h.

Because the time interval between two adjacent tracks is so large (about 72 h), the time autocorrelation

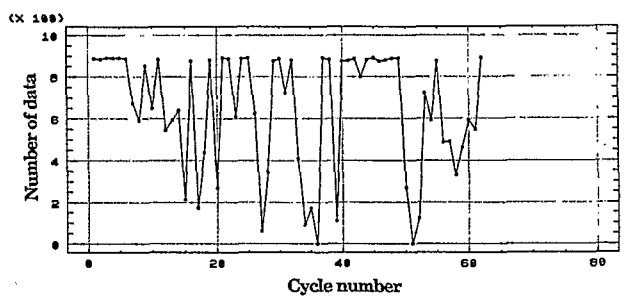

FIG. 3. Number of wind data available along one track for each Geosat cycle, from cycle 1 (October 1986) through cycle 62 (September 1989).

related to Geosat wind data cannot be estimated for small time lags but can only be computed at 0, 72, and 144 h, etc.

A time variogram can be computed based on ship wind data pairs. It is defined as

$$\gamma_{(n\Delta t)} = 1/2E[V_{(x,t)} - V_{(x,t+n\Delta t)}]^2. \quad (2)$$

The time step Δt is 6 h, according to the time interval between two successive synoptic sendings on GTS. This calculation is based on ship wind data pairs separated by a time interval included between $n\Delta t$ and $(n+1)\Delta t$, and by a distance of less than 50 km. This 50-km value is an intermediate choice: it must be large enough for the number of data pairs to be statistically sufficient and small enough to avoid aliasing of spatial variability.

The calculated exponential adjustment of $\gamma(t)$ is

$$\gamma(t) = 3.1 + 5.5(1 - e^{-t/5.2}) \quad (\mathrm{m^2\,s^{-2}}), \quad (3)$$

where t, expressed in 6-h units, ranges from 0 to 5 days ($n = 20$). The value 3.1 appearing at the origin of this experimental variogram is the variance of the in situ error.

The space variograms are defined as follows:

$$\gamma_{(n\Delta x)} = 1/2E[V_{(x,t)} - V_{(x+n\Delta x,t)}]^2. \quad (4)$$

Here, the calculations are independently based on satellite and ship wind data pairs. These pairs are recorded at a given time (in practice, within a 6-h period for ship observations and along individual tracks for Geosat data) and separated by a distance interval included between $n\Delta x$ and $(n+1)\Delta x$.

With an appropriate value of Δx equal to 50 km, the experimental space variograms estimated according to an exponential function between 0 and 1500 km are given by

$$\text{ships:} \quad \gamma(x) = 3.5 + 5.8(1 - e^{-x/15.1}) \quad (\mathrm{m^2\,s^{-2}}), \quad (5)$$

$$\text{Geosat:} \quad \gamma(x) = 0.6 + 5.8(1 - e^{-x/10.4}) \quad (\mathrm{m^2\,s^{-2}}), \quad (6)$$

where x is expressed in 50-km units. Values 3.5 and 0.6 are the variances of in situ and Geosat errors, respectively. In fact, the Geosat error variance is much greater than 0.6 because errors are correlated along a track and for a short distance and do not lead to a visible effect at the origin of the variogram. A fully detailed computation of the Geosat variance error (Muzellec 1991), obtained by analyzing paired ship and satellite data along the Europe–South America shipping route, showed that the true Geosat error variance is approximately equal to 2.9. This variance is composed of two terms: the first [0.6 $\mathrm{m^2\,s^{-2}}$, the value appearing in Eq. (6)] is an estimation of the individual measurement error, whereas the second (2.3 $\mathrm{m^2\,s^{-2}}$) could be related to an along-track error effect due to some systematic problems in wind observation (e.g., a temporary problem with satellite attitude angle, etc.).

Note that the sill values in the experimental space variograms are identical [$\omega = 5.8$ $\mathrm{m^2\,s^{-2}}$ in Eqs. (5) and (6)] and very close to the one in the experimental time variogram ($\omega = 5.5$ $\mathrm{m^2\,s^{-2}}$). The space ranges are somewhat different for ship [$a = 15.1$ in Eq. (5)] and Geosat [$a = 10.4$ in Eq. (6)] data, so that the distance to approach the full space decorrelation by 95% (given as 3 times the value of a) is larger for ships (about 2250 km) than for Geosat (about 1500 km). The time range provided by ship observations [$a/b = 5.2$ in Eq. (3)] gives about a 4-day period to approach the full time decorrelation.

We calculated a space–time experimental variogram $\gamma_{(x,t)}$ obtained by using pairs of in situ data separated by various (x, t) distances. From this 2D variogram and the other 1D variograms defined above [Eqs. (4), (5), and (6)], we adopted the following time–space variogram:

$$\gamma_{(x,t)} = 5.7\left\{1 - \exp\left[-\frac{1}{11}(x + 2.2t)\right]\right\}, \quad (7)$$

where x and t are in 50-km and 6-h units, respectively.

It is to be recalled that this model was constructed from one year of ship and Geosat data in the vicinity of the Europe–South America shipping route from 30°N to 20°S. Because this lane crosses through different wind conditions [strong velocity in the subtropical regions, light velocity close to the intertropical convergence zone (ITCZ)], the model is assumed to be representative of mean annual wind properties in the entire study region. Thus, it has been used for all the kriging calculations that follow.

4. Resulting wind velocity patterns

Wind pattern computations were achieved on a regular 225-km × 225-km grid, very close to the 2° × 2° grid scheme used by SL. For each grid point, the method consisted of integrating the kriging values over a δ-day period. Different wind velocity maps are presented here for a one-month period (December 1986).

A first computation was made on a monthly time scale ($\delta = 31$ days), with reference to wind velocity pattern derived from the previous product proposed by SL. Because SL analysis initially provides monthly pseudostress patterns, such comparison must be made with some cautions (Hanawa and Taba 1987). Despite this remark, the two monthly wind patterns were quite similar (Figs. 4a and 4b) both for amplitude and the space gradient. The highest values ($V > 9$ m s^{-1}) for both studies relate to the core of the northeast trade system (10°N, 45°W). Another region with secondary high values ($V > 7$ m s^{-1}) corresponds to the core of the southeast trade system (10°S, 25°W). The weakest wind velocity values ($V < 6$ m s^{-1}) were correctly noted in the Gulf of Guinea, particularly in the region of the

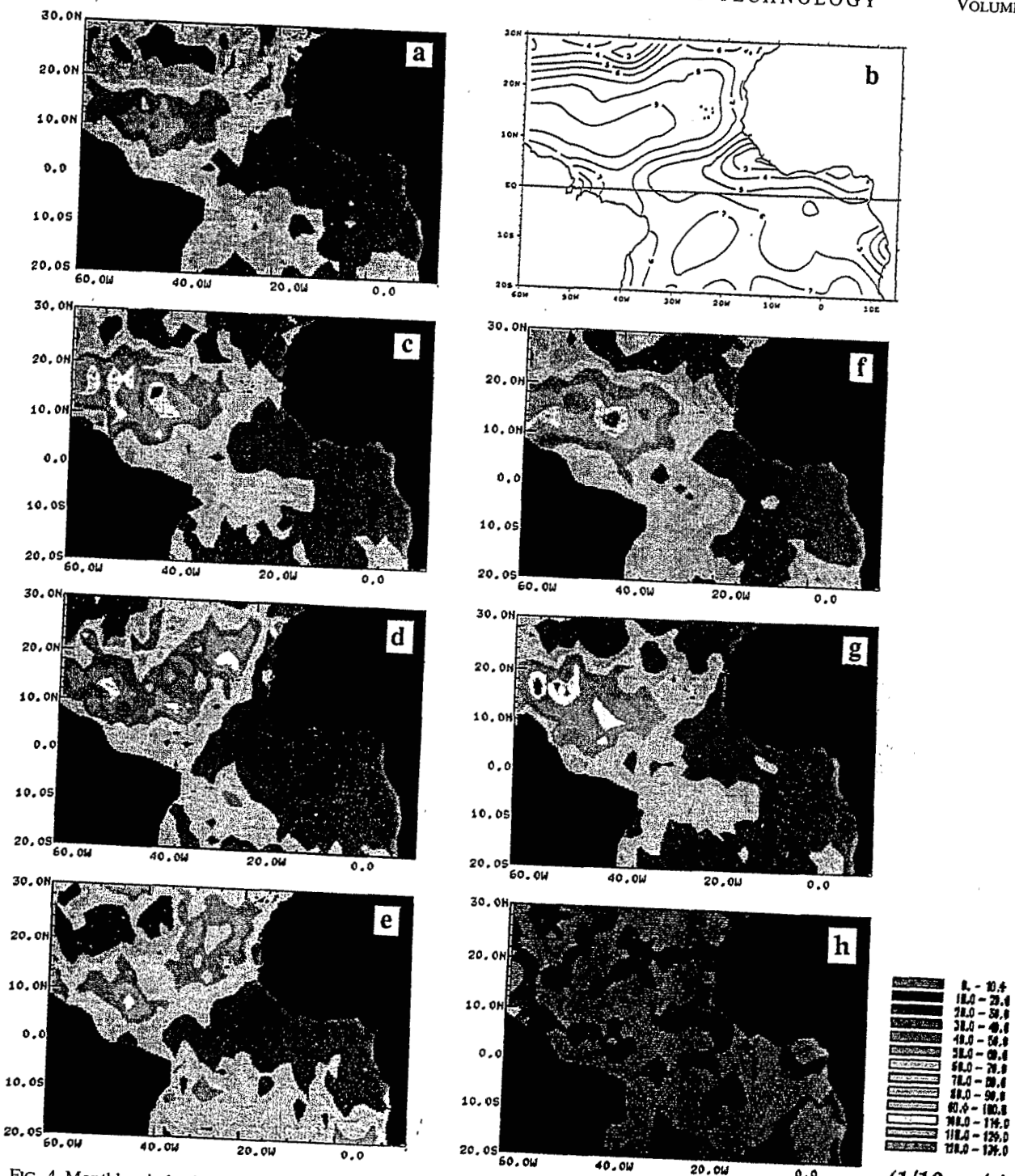

FIG. 4. Monthly wind velocity patterns (m s^{-1}) for December 1986: (a) derived from combined Geosat–ship data; (b) derived from SL analysis, using only ship data. The three sequential 10-day integrated wind velocity patterns (m s^{-1}) for December 1986 derived from combined Geosat–ship data: (c) days 1–10; (d) days 11–20; (e) days 21–31. First 10-day integrated wind velocity patterns (m s^{-1}) for December 1986: (f) derived from ship data only; (g) derived from Geosat data only; (h) absolute difference between ship data analysis and Geosat data analysis.

ITCZ off the African coast. Light wind also occurred in the northern (22°–30°N) and southern (18°–20°S) limits of the domain.

One main objective of our study was to decrease the δ period to less than one month. We chose $\delta = 10$ days, a value that should be compared to the 17-day Geosat cycle during ERM. Three sequential 10-day integrations were performed, combining the two types of wind data relative to December 1986. Kriging value was determined for each node, using the 24 closest observations independently of data source, though after resampling of satellite data in an effort to avoid a high density of measurements along the satellite track. To preserve temporal symmetry, we added a constraint, that is, the extraction of half this number during each 5-day period in the middle of each 10-day period. Figures 4c, 4d, and 4e show detailed space–time changes in wind velocity during December 1986. The range of values obtained by 10-day ship–satellite computation ($1 \text{ m s}^{-1} < V < 12 \text{ m s}^{-1}$) was considerably greater than that obtained by monthly ship–satellite calculation ($3 \text{ m s}^{-1} < V < 10 \text{ m s}^{-1}$). The area with the highest values in the northeast trade-wind sector showed a gradual reduction from the first to the third 10-day period. Meanwhile, the southeast trade winds steadily increased. Other variations were noted in the Gulf of Guinea (lighter winds during the second 10-day period) and in regions close to the northern and southern limits.

To evaluate our kriging method, we performed the same analysis for each of the 10-day periods during December 1986, but used either Geosat measurements only or ship observations only. The exceptionally large number of ship observations available during December 1986 (20% more than the monthly mean) facilitated such analysis. We show in Figs. 4f and 4g the wind patterns of the first 10-day period for ship and Geosat data, respectively. Figure 4h is related to their absolute differences. Discussion about the results for the two other 10-day periods would be analogous. The ship and Geosat wind patterns should be compared with each other and considered in relation to Fig. 4c, related to the combined analysis. In fact, the resulting patterns were quite similar, and the absolute differences were on the whole within about 1 m s^{-1}. Furthermore, no systematic arrangement, related for instance to satellite tracks or shipping routes, was noted in the difference patterns. The extremes of wind velocity were comparable, both for spatial distribution and force. Nevertheless, Geosat data seem to amplify the contrasts slightly: Satellite strong (or light) wind velocities were generally higher (or lower) than those of ship observations. This last result, previously noted by Etcheto and Banège (1992), could be explained by the fact that ship wind speed has a tendency to be high at low wind speed and low at high wind speed (Pierson 1990). The wind pattern obtained by our combined analysis (Fig. 4c) was obviously a compromise between satellite and ship wind patterns, although closer to the Geosat pattern because of the greater number of satellite measurements (three Geosat measurements for one ship observation on average).

5. Conclusions

Future climatic research will require observation of synoptic wind patterns, especially over oceanic domains. The determination of such patterns remains uncertain when only in situ observations provided by merchant ships are used. A new possibility is to use wind information provided by satellite measurements. Our main objective in this paper was to suggest combining ship and satellite datasets. For that purpose we used wind data provided both by ships of opportunity and Geosat altimeter readings over the tropical Atlantic Ocean.

The kriging method appears to be an interesting means of combining the two data sources on a regular $2° \times 2°$ grid. Because of the high density of the mutual database, the wind pattern can be integrated over a 10-day period, that is, a time span three times shorter than usual with ship data only. This approach should provide better understanding of changes in climatic events over time and an appreciable improvement in the accuracy of dynamic forcing in oceanic numerical experiments.

The present work was undertaken as a pilot study. Consequently, not all problems were investigated. To improve the demonstration, specific features need to be considered. A more extensive study of the choice of the neighboring observations used to calculate the kriging value at each grid point is required. It would also be of interest to take the spatial anisotropy of the wind into account in computing variogram coefficients. Moreover, the integration step (a 10-day period here), as well as the grid scheme, should be chosen to optimize the procedure.

We analyzed only the modulus of the wind since wind direction cannot be determined by the Geosat altimeter. Both the modulus and wind direction can be estimated thanks to a scatterometer such as that of *ERS-1*, a satellite launched in July 1991. Based on a sample of a few days of wind data from the *ERS-1* scatterometer, an initial test (Le Naour 1992, personal communication) demonstrated that the kriging method can also be used for each wind component. A refinement of our method combining wind vectors provided both by this scatterometer and ships of opportunity is in progress. This study will include all the features noted above that were not investigated in the present work.

Acknowledgments. The authors wish to thank J. F. Minster and C. Brossier of GRGS (Toulouse, France) for providing an appropriate selection of satellite data,

and J. O'Brien, D. Legler, and J. Stricherz of MASIG-FSU (Tallahassee, Florida) for supplying raw in situ data on a regular basis. The computational work was performed while A. Muzellec was at the ORSTOM Centre in Brest. Comments by J. F. Minster and D. Legler were useful for improvement of the manuscript. This research was partly funded by ORSTOM, IFREMER, and the French PNEDC.

REFERENCES

Andrich, P., P. Delecluse, C. Levy, and G. Madec, 1988: A multitasked general circulation model of the ocean. *Science and Engineering on Cray Supercomputers,* Cray Research Inc., 407–428.

Arnault, S., L. Gourdeau, and Y. Menard, 1992: Comparison of the altimetric signal with in situ measurements in the tropical Atlantic Ocean. *Deep-Sea Res.*, **39,** 481–499.

BOAT's collection, 1990–91: Bulletin Océan Atlantique Tropical. A contribution to Program TOGA/France, Vols. 1 and 2, Programme National d'Etude de la Dynamique du Climat, Centre ORSTOM.

Boutin, J., 1990: Utilisation et validation des vents satellitaires pour l'étude à l'échelle globale de l'échange du gaz carbonique entre l'océan et l'atmosphère. *Thèse de l'Université de Paris VII,* 94 pp.

Brown, G. S., 1979: Estimation of surface winds using satellite-borne radar measurements at normal incidence. *J. Geophys. Res.*, **84,** 3974–3978.

Chelton, D. B., and F. J. Wentz, 1986: Further development of an improved wind speed algorithm. *J. Geophys. Res.*, **91,** 14 250–14 260.

Cheney, R. E., B. C. Douglas, R. W. Agreen, L. Miller, D. L. Porter, and N. S. Doyle, 1987: Geosat altimeter geophysical data record user handbook. NOAA Tech. Memo. NOS NGS-46, Natl. Geod. Surv., Rockville, MD, 32 pp.

Dobson, E. B., F. Monaldo, J. Goldhirst, and J. Wilkerson, 1987: Validation of Geosat altimeter-derived wind speeds and significant wave heights using buoy data. *J. Geophys. Res.*, **92,** 10 719–10 731.

Etcheto, J., and L. Banège, 1992: Wide-scale validation of Geosat altimeter-derived wind speed. *J. Geophys. Res.*, **97,** 11 393–11 409.

Gohin, F., and G. Langlois, 1993: Using geostatistics to merge in situ measurements and remotely sensored observations of sea surface temperature. *Int. J. Remote Sens.*, **14,** 9–19.

Goldhirst, J., and E. B. Dobson, 1985: A recommended algorithm for the determination of ocean surface wind speed using a satellite-borne radar altimeter. Rep. JHU/APL SIR-85-U005, John Hopkins Univ., Appl. Phys. Lab., Laurel, MD.

Hanawa, K., and Y. Toba, 1987: Critical examination of estimation methods of long-term mean air–sea heat and momentum transfers. *Ocean–Air Interactions J.*, **1,** 79–93.

Matheron, G., 1971: The theory of regionalized variables and its applications. Tech. Rep. Fascicule 5, Les cahiers du Centre de Morphologie Mathématique de Fontainebleau, Ecole Supérieure des Mines, Paris, 212 pp.

Morlière, A., and C. Duchêne, 1990: Evaluation des courants de surface d'un modèle de circulation générale de l'Atlantique tropical. Rap. Interne LODYC, 90/11, Université P. et M. Curie, Paris, 32 pp.

Muzellec, A., 1991: Apport de vents altimétriques GEOSAT à la détermination des champs de vent dans l'Atlantique tropical. Doc. Scient. ORSTOM-Brest No. 59, Centre ORSTOM, BP 70, 29280 Plouzané, France, 87 pp.

Olea, R. A., 1974: Optimal contour mapping using universal kriging. *J. Geophys. Res.*, **79,** 695–702.

Picaut, J., J. Servain, A. J. Busalacchi, and M. Séva, 1984: Interannual variability versus seasonal variability in the tropical Atlantic. *Geophys. Res. Lett.*, **11,** 787–790.

——, ——, P. Lecomte, M. Séva, S. Lukas, and G. Rougier, 1985: Climatic atlas of the tropical Atlantic wind stress and sea surface temperature 1964–1979. Université de Bretagne Occidentale, Brest–University of Hawaii, Honolulu, 467 pp.

Pierson, Jr., W. J., 1990: Examples of, reasons for, and consequences of the poor quality of wind data from ships for the marine boundary layer: Inapplications for remote sensing. *J. Geophys. Res.*, **95,** 13 313–13 340.

Servain, J., 1990: Near real-time sea surface temperature and wind stress analysis for the tropical Atlantic Ocean. *Trop. Ocean-Atmos. Newslett.*, **54,** 4–6.

——, and D. M. Legler, 1986: Empirical orthogonal function analyses of tropical Atlantic sea surface temperature and wind stress 1964–1979. *J. Geophys. Res.*, **91,** 14 181–14 191.

——, and S. Lukas, 1990: *Climatic Atlas of the Tropical Atlantic Wind Stress and Sea Surface Temperature:* 1985–1989. SDP IFREMER, 143 pp.

——, A. Morlière, and C. S. Pereira, 1992: Simulated versus observed sea surface temperature in the tropical Atlantic Ocean. *The Ocean Atmosphere System,* Gordon and Breach, in press.

——, M. Séva, S. Lukas, and G. Rougier, 1987: Climatic atlas of the tropical Atlantic wind stress and sea surface temperature: 1980–1984. *Ocean–Air Interactions J.*, **1,** 109–192.

Witter, D. L., and D. B. Chelton, 1991: A Geosat altimeter wind speed algorithm and a method for altimeter wind speed algorithm developments. *J. Geophys. Res.*, **96,** 8853–8860.

Reprinted from JOURNAL OF ATMOSPHERIC AND OCEANIC TECHNOLOGY, Vol. 10, No. 6, December 1993
American Meteorological Society

Wind Fields at the Sea Surface Determined from Combined Ship and Satellite Altimeter Data

JACQUES SERVAIN

FRANCIS GOHIN

ALAIN MUZELLEC